Available online at www.sciencedirect.com
SCIENCE DIRECT®
Organic Electronics 5 (2004) 309–314
Organic Electronics
www.elsevier.com/locate/orgel

Spin polarised electrodes for organic light emitting diodes

I. Bergenti [a,*], V. Dediu [a], E. Arisi [a], T. Mertelj [a,b], M. Murgia [a], A. Riminucci [a], G. Ruani [a], M. Solzi [c], C. Taliani [a]

[a] *Istituto per lo Studio dei Materiali Nanostrutturati ISMN sez. Bologna, via Gobetti 101, 40129 Bologna, Italy*
[b] *University of Ljubljana, Faculty of Mathematics and Physics, Jadranska 19, 1000 Ljubljana, Slovenia*
[c] *University of Parma, Faculty of Physics and INFMParco Area delle Scienze 7/a, 43100 Parma, Italy*

Received 15 October 2003; received in revised form 2 August 2004; accepted 19 October 2004
Available online 18 November 2004

Abstract

Electroluminescence in organic semiconductors strongly depends on the relative population of singlet and triplet excitonic states, i.e. on the carrier spin statistics. In conventional organic light-emitting diodes (OLED) the optical emission is usually based on fluorescence from excited singlet states, while triplet states provide phosphorescent radiation. Radiative emission from singlet excitons has a very large transition probability providing the main radiative pathway. Quantum constraints determine the statistics of singlet–triplet exciton formation from charge recombination to a 1:3 partition. Controlling the spin statistics by injecting carriers with the desired spin polarisation would open the way to enhance a chosen electronic transition and therefore increase the device efficiency.

We show that spin polarised materials can successfully replace conventional electrodes in OLEDs. Electrical and optical characterisations of Alq_3/TPD based OLEDs for both normal and spin polarised electrodes are presented. Epitaxial thin films of the manganite $La_{0.7}Sr_{0.3}MnO_3$ were used as spin polarised hole injectors, while iron and cobalt films were used as spin polarised electron injectors. The results are a first step towards the fabrication of devices where the light emission can be tuned by controlling the spin injection.

PACS: 72.25.Hg; 75.47.Lx; 78.60.Fi
Keywords: Spin polarised injection; Organic light emitting diode; Manganites

1. Introduction

The spin statistics of carrier recombination in organic semiconductors is attracting the interest of many researchers due to both fundamental and application aspects. Electroluminescence in

* Corresponding author. Tel.: +39 051 6398517; fax: +39 051 6398539.
E-mail address: i.bergenti@ism.bo.cnr.it (I. Bergenti).

1566-1199/$ - see front matter © 2004 Elsevier B.V. All rights reserved.
doi:10.1016/j.orgel.2004.10.004

organic light emitting diodes (OLED) is mainly based on the radiative decay of singlet excitons [1] which are usually created by injecting electrons (e) and holes (p) from separate electrodes. The singlet/triplet partition is determined by quantum statistics as 1:3, taking into account a similar formation probability for one singlet and three triplet states. This probability is a topic of many investigations and some recent works [2,3] indicate a higher formation cross-section for singlet states in some materials although this issue is still highly debated by scientific community. The use of spin polarised (SP) injection in OLEDs should in principle help to overcome the 1:3 statistics constraints. Significant SP injection from ferromagnetic materials into π-conjugated oligomers has been recently demonstrated [4–6].

The effect of the SP injection on the exciton formation can be easily understood on the basis of simple considerations. In the case of non SP injection (all e↑, e↓, p↑ and p↓ carriers are present), two electrons and two holes can in general combine in four different pairs: e↑p↑, e↑p↓, e↓p↑, e↓p↓. To the first approximation, the parallel states do not contribute to light emission, while the antiparallel ones do contribute with some finite probability. In the singlet–triplet fashion any antiparallel pair corresponds to 1/2(S + T) and the four pairs provide one singlet and three triplet states, leading to the well known 1/4 probability for singlet formation:

$$\begin{aligned} &\mathrm{e}\uparrow \mathrm{p}\uparrow + \mathrm{e}\uparrow \mathrm{p}\downarrow + \mathrm{e}\downarrow \mathrm{p}\uparrow + \mathrm{e}\downarrow \mathrm{p}\downarrow \\ &\quad = T + 1/2(S+T) + 1/2(S+T) + T \\ &\quad = S + 3T \end{aligned} \tag{1}$$

In case of one spin polarised electrode (e↑, p↑ and p↓ only carriers present) one has

$$\begin{aligned} &\mathrm{e}\uparrow \mathrm{p}\uparrow + \mathrm{e}\uparrow \mathrm{p}\downarrow = T + 1/2(S+T) \\ &\quad = 1/2S + 3/2T \end{aligned} \tag{2}$$

The sum (2) provides the same singlet/triplet ratio, indicating no effect for only one SP electrode. Nevertheless this consideration is not completely straightforward, because of possible spin filtering effects by SP electrode.

If both spin polarised electrodes are aligned in the antiparallel way, we can consider the e↑, p↓ case, as the most favourable for singlet formation:

$$\mathrm{e}\uparrow \mathrm{p}\downarrow = 1/2(S+T) = 1/2S + 1/2T \tag{3}$$

With such an injection it should be possible to double the efficiency compared to conventional singlet based OLEDs.

For the parallel alignment the e↑ p↑ or e↓ p↓ would generate only triplet states. Thus, in addition to the efficiency enhancement, the control of the spin statistics should give the possibility of switching from singlet to triplet operation [7].

In this article we present experimental results that indicate that efficient OLEDs can be fabricated by replacing ITO with nearly 100% spin polarised manganite (hole injecting electrode) and by replacing Al with nearly 30% spin polarised Co and Fe.

2. Experimental

The $La_{1-x}Sr_xMnO_3$ manganites are characterised by unusual electrical and magnetic properties depending on the doping fraction x [8]. $La_{0.7}Sr_{0.3}MnO_3$ (LSMO) is a metallic ferromagnet at room temperature (Curie temperature $T_C = 370\,K$) characterised by a relatively small density ($\sim 10^{21}$–$10^{22}\,cm^{-3}$) of highly spin polarised charge carriers [9]. Epitaxial films of LSMO were grown on (1 0 0) oriented transparent $SrTiO_3$ (STO) substrates by Channel–Spark ablation (CSA) from polycrystalline targets [10]. LSMO targets were synthesised by high temperature (1200 °C) solid state reaction from La_2O_3, $SrCO_3$ and MnO_2 powders in the stoichiometric ratio. The oxygen pressure was kept constant during the deposition process ($P = 2.5 \times 10^{-2}$ mbar) and the STO substrate temperature was about 1150 K. The film thicknesses were measured by a conventional α-step technique, and the resistance was checked by the four point technique in the 10–300 K temperature range. Transmittance of manganite films in the visible range have been measured by the JASCO V550, a double beam spectrophotometer equipped with a monochromator and photomultiplier tube detector.

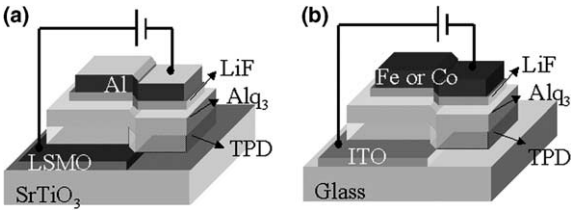

Fig. 1. A schematic diagram of the OLED devices: (a) **LSMO**/TPD/Alq_3/LiF/**Al** (**LSMO–Al**), (b) **ITO**/TPD/Alq_3/LiF/**Fe** or **Co** (**ITO–Fe** and **ITO–Co**).

Three different OLED geometries with SP electrodes were fabricated: **LSMO**/TPD/Alq_3/LiF/**Al** (**LSMO–Al**), **ITO**/TPD/Alq_3/LiF/**Fe** (**ITO–Fe**) and **ITO**/TPD/Alq_3/LiF/Al/**Co** (**ITO–Co**) (see Fig. 1). The SP OLEDs behaviour was compared to that of "standard" **ITO**/TPD/Alq_3/LiF/**Al** (**ITO–Al**) OLEDs. Organic films, N,N′-diphenyl-N,N′-(3-methylphenyl)-1,1′-biphenyl-4,4′diamine (TPD) and 8-hydroxyquinoline Aluminium (Alq_3), were deposited by sublimation of highly purified compounds in UHV (10^{-10} mbar) molecular beam deposition chamber. TPD acts as a hole conducting layer. There is no significant electron transport across it, what confines the electron–hole recombination in the electroluminescent Alq_3 material near the interface with the TPD layer.

For **LSMO–Al** devices, different organic film thicknesses were investigated for both TPD and Alq_3: 35 nm TPD/35 nm Alq_3, 35 nm TPD/70 nm Alq_3, 70 nm TPD/35 nm Alq_3 and 70 nm TPD/70 nm Alq_3. In **ITO–Co** OLEDs the TPD and Alq_3 layers were both 150 nm thick, for **ITO–Fe** OLEDs 35 nm and 80 nm and **ITO–Al** OLEDs 35 nm and 70 nm respectively. The top contacts (50 nm thick Al, Co and Fe) were deposited by sublimation from Al_2O_3 crucible of high purity compound at a pressure of about 10^{-6} mbar. The sample-crucible distance was 30 cm and the deposition rate was 0.1 nm/s. A LiF thin layer of about 2 nm is known to considerably improve OLED performances [11] when placed between Alq_3 and the cathode, and this effect was confirmed in investigated SP OLEDs. A 1 nm thick Al layer was deposited underneath Co electrode in the **ITO–Co** OLEDs in order to prevent the penetration of highly energetic Co atoms in the organic layers during the deposition. Moreover, the Al layer was found to decrease the device turn-on voltage. The spin injection across thin non magnetic metal barriers does not significantly decrease the spin polarisation as demonstrated in different spintronic devices [12,13].

Detailed magnetic characterisation of the manganite and Co films was performed by a variety of methods, including SQUID magnetometry, ac-susceptibility, X-ray magnetic dichroism, Kerr effect and others.

The *I–V* curves were collected by Keithley 236 source meter unit. The emitted light was analysed by the optical multichannel analyser Hamamatsu PMA-11 via an optical fibre placed in front of the transparent substrate. The spectra were subsequently corrected for instrumental response and for the transmission spectra of ITO–glass and LSMO–$SrTiO_3$ respectively.

3. Results and discussion

The optical transmittance for LSMO thin films of different thicknesses is shown in Fig. 2. The transmittance is flat in the 400–850 nm range and is as high as 60% for the 12 nm thick sample. The samples are metallic at room temperature with a resistivity of about 10 mΩcm. The Curie

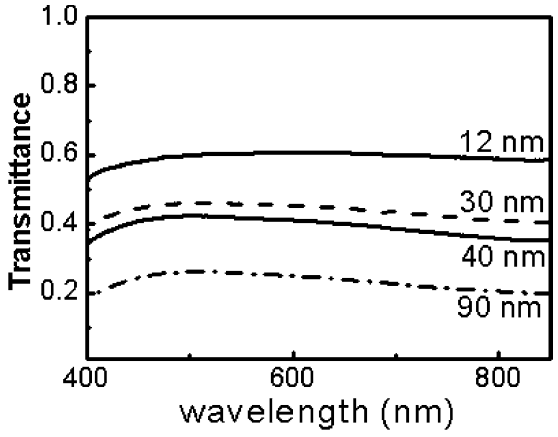

Fig. 2. Transmittance in the visible range corresponding to manganite thin films of different thicknesses deposited on STO single crystals.

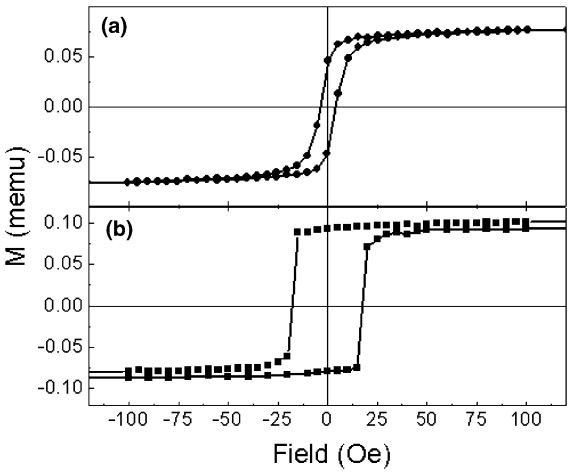

Fig. 3. Hysteresis loop with external magnetic field applied in plane for (a) 20 nm thick LSMO on STO and (b) 50 nm thick Co on STO/TPD/Alq_3.

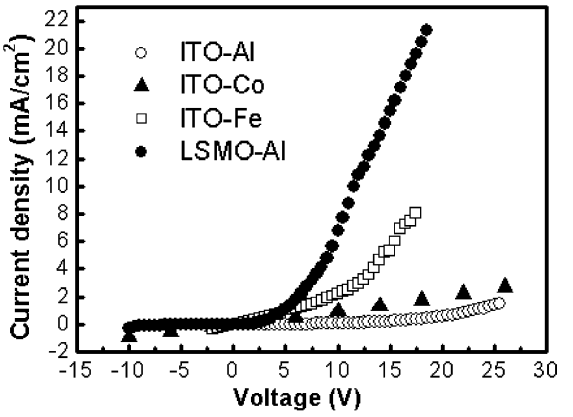

Fig. 4. IV curves for **LSMO**/TPD (70 nm)/Alq_3 (70 nm)/LiF/**Al**(●), **ITO**/TPD(35 nm)/Alq_3 (80 nm)/LiF/**Fe** (□) and **ITO**/TPD(150 nm)/Alq_3 (150 nm)/LiF/Al/**Co**(▲) OLEDs together with the **ITO**/TPD(35 nm)/Alq_3 (70 nm)/LiF/**Al** reference device (○).

temperature defined from magnetisation measurements is between 320 and 360 K depending on the film thickness. Fig. 3(a) shows the hysteresis loop measured by a SQUID magnetometer for a 20 nm thick film at 300 K in a parallel magnetic field. The coercive field is about 4 Oe. Surface properties were investigated by XPS and UPS [14]. The results confirm ferromagnetic metallic nature of LSMO films providing important information on their electronic structure and work function. These findings indicate that the ferromagnetic spin-polarised LSMO thin films deposited on a $SrTiO_3$ combine strong ferromagnetic state and high carrier spin polarisation with significant optical transparency in the visible range and can be used in the electro-optical devices with performances similar to conventional transparent electrodes.

The LSMO film thickness was kept between 10 nm and 20 nm for all the investigated devices. The magnetic properties of the Co top electrode were investigated in a OLED-like geometry. 50 nm Co thin films were evaporated on top of TPD/Alq_3 organic bilayers which were deposited on a STO substrate (STO/TPD/Alq_3/**Co**). The organic bilayer thickness was similar to that of the OLED devices. Although the soft organic underlayers modify considerably the structural and magnetic properties of the Co layer, it is clearly ferromagnetic at 300 K as shown in Fig. 3(b). The coercive field of about 20 Oe and the square-like hysteresis loop indicate the high magnetic quality of such films. One can in principle expect similar behaviour for the Fe films, taking into account many common features for these two metals.

Typical *I–V* curves for SP OLEDs in **LSMO–Al**, **ITO–Co** and **ITO–Fe** geometries are shown in Fig. 4. The *I–V* characteristic of a **ITO–Al** device is also shown for comparison. The **LSMO–Al** curve is rather asymmetric, showing a rectification coefficient of about 50. The current density of LSMO based OLEDs with the thickest organic bilayer (70 nm for both TPD and Alq_3) is two orders of magnitude higher than a conventional **ITO–Al** OLEDs with the same rectification properties [11]. This difference cannot be explained by better electronic level alignment at the interface. The manganite work function ϕ_{LSMO} is about 4.7–4.8 eV [14] and is similar to that of ITO ($\phi_{ITO} \sim 4.8$ eV) (see Fig. 5). The most plausible explanation is the presence of parallel conduction channels. This hypothesis is supported by AFM studies which show the presence of sharp outgrowths on manganite films whose density increases with the film thickness (to be published elsewhere). The presence of these defects can generate pinholes and affect the OLED characteristic. This scenario is also supported by relatively low

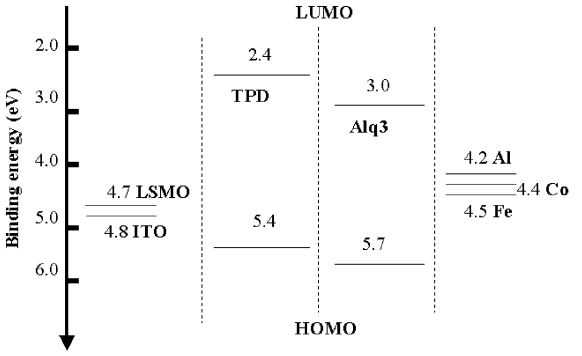

Fig. 5. Fermi levels and HOMO/LUMO energy levels alignment for the materials used in the analysed OLEDs.

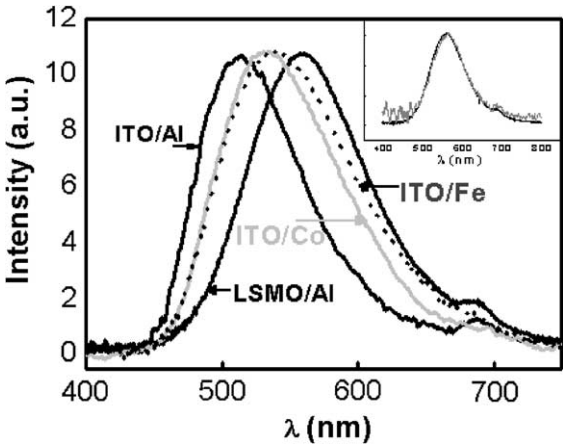

Fig. 6. Electroluminescence spectra corrected for substrate transmission and CCD camera response. The inset shows the collected spectra for the **LSMO–Al** OLED in parallel external magnetic field of 0.35 T (black line) and at $H = 0$ (grey line).

electroluminescence efficiency in comparison with the **ITO–Al** device. The increase in current density is also found in **ITO–Co** and **ITO–Fe** OLEDs. The presence of pinhole-like defects generated by the penetration of high energy Co and Fe atoms in the organic materials during the metal deposition has to be investigated in more detail.

The **ITO–Co** OLEDs display a ohmic behaviour in the low voltage range (below 10 V) indicating the presence of high resistivity parallel conduction channels. Typical exponential diode behaviour is evident above the electroemission threshold voltage (about 25 V). This behaviour can be understood on the basis of work function alignment (Fig. 5). The Co work function [15] ($\phi_{Co} \sim 4.4$ eV) is higher than that of Al ($\phi_{Al} \sim 4.2$ eV) leading to a lower I–V asymmetry with respect to the **ITO–Al** devices. On the other hand, we cannot exclude variations of the Co work function value depending on the growth conditions and on the crystallographic order of the evaporated thin films.

The electrical behaviour of the **ITO–Fe** devices is similar to that of the **ITO–Co** devices except for the lower electroemission threshold voltage (7 V) in the former. It should be noted that due to the high Fe reactivity with oxygen, **ITO–Fe** OLED was measured in Ultra High Vacuum immediately after deposition. This makes it difficult to compare the behaviour of this OLED with that of the others.

For all the OLEDs, the detected EL spectra correspond to the Alq_3 emission. Fig. 6 shows the spectra for the three studied SP OLEDs. The spectrum of a standard **ITO–Al** device is also shown as a reference. The spectrum of the **ITO–Al** OLED has the maximum at approximately 515 nm. This value is similar to that reported in most of the literature on Alq_3 based OLEDs and generally does not depend on cathode material. As it can be seen from Fig. 6 all the SP OLED spectra are shifted to longer wavelengths. **ITO–Fe** and **ITO–Co** spectra are quite similar in the high energy part while the **ITO–Fe** one is broader in the red region.

The strongest red shift was consistently found in **LSMO–Al** OLEDs. It is important to note that for the **LSMO–Al** devices the shift was not dependent on the thicknesses of the separate organic layers. The same shift was observed in devices with the four different TPD/Alq_3 thickness combinations.

At the moment we cannot ascribe the observed shift to the spin polarised injection of carriers. Smaller red shifts have been reported in literature for OLEDs with non spin polarised electrodes. Its presence was associated to several factors, such as the presence of impurities, the increase of current density across the device [16] or the material disorder. In our case, growth conditions ensure highly pure electroluminescent materials and, on the other hand, increasing the current across the device did not cause the peak positions to vary significantly.

The external magnetic field does not influence in a detectable way the EL spectra of the **LSMO–Al** based OLEDs as shown in the inset in Fig. 6. Such a result is quite obvious for OLEDs with one SP electrode: the external magnetic field just orients in the same direction the magnetic domains in LSMO, while each separate domain will form a small (one electrode) SP OLED. The optical behaviour of the resulting small SP OLED does not depend on the magnetic orientation of the domains in the neighbourhood. The magnetic field is expected, on the other hand, to have a strong effect on OLEDs with two SP electrodes.

4. Conclusions

The electroluminescence of TPD/Alq_3 based OLEDs with novel spin polarised ferromagnetic electrodes has been investigated.

Semitransparent thin films of highly polarised LSMO manganite deposited on $SrTiO_3$ were used as hole injectors with performances similar to conventional transparent electrodes. Ferromagnetic top electrodes of Co and Fe layers were found to act as a appropriate electron injectors. The electrical and optical behaviour of SP OLEDs have been found to be quite similar to that with non-ferromagnetic electrodes while some unusual spectral behaviour has yet to be understood.

Acknowledgements

The authors want to acknowledge the partial support of this work from EC Network Projects STEPLED IST-2001-37375 and SPINOSA IST-2001-33334 and from FIRB ''Microsistemi e Nanomateriali Magnetici'' and FIRB ''Nanotecnologie e nanodispositivi per la società dell' informazione''.

References

[1] R. Friend, R.W. Gymer, A.B. Holmes, J.H. Burroughes, R.N. Marks, C. Taliani, D.D.C. Bradley, D.A. Dos Santos, J.L. Brédas, M. Lögdlund, W.R. Salaneck, Nature 397 (1999) 121.
[2] Y. Cao, I.D. Parker, G. Yu, C. Zhang, A.J. Heeger, Nature 397 (1999) 414.
[3] M. Wohlgenannt, X.M. Jiang, Z.V. Vardeny, R.A.J. Janssen, Phys. Rev. Lett. 88 (2002) 197401.
[4] V. Dediu, M. Murgia, F.C. Matacotta, C. Taliani, S. Barabanera, Solid State Commun. 122 (2002) 181.
[5] Z.H. Xiong, D. Wu, Z.V. Vardeny, J. Shi, Nature 427 (2004) 821.
[6] E. Arisi, I. Bergenti, V. Dediu, M.A. Loi, M. Muccini, M. Murgia, G. Ruani, C. Taliani, R. Zamboni, J. Appl. Phys. 93 (2003) 7682.
[7] M.A. Baldo, S.P. Lamansky, E. Burrows, M.E. Thompson, S.R. Forrest, Appl. Phys. Lett. 75 (1999) 4.
[8] A.J. Millis, Nature 392 (1998) 147.
[9] J.E. Núñez-Regueiro, D. Gupta, A.M. Kadin, J. Appl. Phys. 79 (1996) 5179.
[10] V. Dediu, J. Lopez, M.F.C.P. Nozar, G. Ruani, R. Zamboni, C. Taliani, Phys. Status Solidi B 215 (1999) 625.
[11] C.W. Tang, S.A. VanSlike, C.H. Chen, J. Appl. Phys. 65 (1989) 3610.
[12] M. Johnson, Phys. Rev. Lett. 70 (1993) 2142.
[13] R. Jansen, H. Gokcan, O.M.J. van't Erve, F.M. Postma, J.C. Lodder, J. Appl. Phys. 95 (2004) 6927.
[14] M.P. de Jong, V.A. Dediu, C. Taliani, W.R. Salaneck, J. Appl. Phys. 94 (2003) 7292.
[15] R.C. Weasts, Handbook of Chemistry and Physics, The Chemic Rubber Co, Cleveland, 1971.
[16] D.M. Shin, S.T. Lim, J.S. Choi, J.S. Kim, Thin Solid Films 363 (2000) 268.